

# Synthesis, Structure, and Thermal Stability of $\text{Li}_3\text{AlB}_2\text{O}_6$

M. He,\* X. L. Chen,\*<sup>1</sup> V. Gramlich,<sup>†</sup> Ch. Baerlocher,<sup>†</sup> T. Zhou,\* and B. Q. Hu\*

\*Institute of Physics and Center for Condensed Matter Physics, Chinese Academy of Sciences, P. O. Box 603, Beijing 100080, People's Republic of China; and <sup>†</sup>Laboratory of Crystallography, ETH, Ch-8092, Zurich, Switzerland

Received May 15, 2001; in revised from August 13, 2001; accepted August 17, 2001

A new compound,  $\text{Li}_3\text{AlB}_2\text{O}_6$ , has been synthesized by solid state reaction and its structure has been solved and refined from single-crystal and power X-ray diffraction data. This compound crystallizes in a triclinic unit cell (space group  $P\bar{1}$ ) with lattice parameters  $a = 4.876(8)$  Å,  $b = 6.191(16)$  Å,  $c = 7.910(20)$  Å,  $\alpha = 74.46(18)^\circ$ ,  $\beta = 89.44(17)^\circ$ , and  $\gamma = 89.52(18)^\circ$ . There are 2 formulas per unit cell and 12 atoms in the asymmetric unit. This structure is built up of infinite  $[\text{Al}_2(\text{BO}_3)_4]_\infty^{6-}$  complex chains that are parallel to the  $a$  axis and separated by Li atoms. Although this structure exhibits many structural similarities to a previously reported compound with the same chemical composition, its unit cell and its powder diffraction pattern are different and so is the distribution of the Li atoms. Infrared and thermal analyses were also performed to compare with previous reports. © 2002 Elsevier Science (USA)

**Key Words:** aluminum borate; structure; thermal stability.

## 1. INTRODUCTION

In the past decades much research interest has been focused on the synthesis and characterization of inorganic borates for the exploration of nonlinear optical materials. Besides the well-known binary borates, such as  $\beta\text{-BaB}_2\text{O}_4$  (1),  $\text{LiB}_3\text{O}_5$  (2), and  $\text{CsB}_3\text{O}_5$  (3), many ternary borates have recently been synthesized and structurally characterized.  $\text{Sr}_2\text{Be}_2\text{B}_2\text{O}_7$  (4) and  $\text{K}_2\text{Al}_2\text{B}_2\text{O}_7$  (5) are successful examples of exploring new optical materials in ternary borate.

$\text{Li}_2\text{O}-\text{Al}_2\text{O}_3-\text{B}_2\text{O}_3$  is an especially interesting ternary system to explore for new compounds with potential functions. Al has an outer electronic structure similar to that of B and is often in tetra coordination so it may act like a tetrahedrally coordinated B.

The  $\text{Li}_2\text{O}-\text{Al}_2\text{O}_3-\text{B}_2\text{O}_3$  system has indeed attracted the attention of researchers for a very long time. Kim and Hummel (6) investigated this system already in 1962 and reported two ternary borates,  $\text{Li}_4\text{Al}_4\text{B}_6\text{O}_{17}$  and  $\text{Li}_2\text{AlBO}_4$ .

In 1983, Abdullaev *et al.* studied this system in more detail (7). Although many ternary borates were reported by Abdullaev *et al.*, only  $\text{Li}_3\text{AlB}_2\text{O}_6$  was structurally characterized (8,9). Another compound,  $\text{LiAl}_7\text{B}_4\text{O}_{17}$ , was reported by Åhman *et al.* (10) in 1997.  $\text{Li}_3\text{AlB}_2\text{O}_6$  was found to be triclinic, space group  $P\bar{1}$ . However, bond valence calculations revealed that the sum of the bond valences for Al is only about 2.11, which is much lower than the normal oxidation state. Moreover, a strong reflection in the powder diffraction pattern of this compound by the same author (7) cannot be indexed with their unit cell. In 1997, Chrysikos *et al.* (11) confirmed the existence of  $\text{Li}_3\text{AlB}_2\text{O}_6$  and reported its infrared and Raman spectra. But they obtained different results for the thermal stability of this compound. Abdullaev *et al.* (7) reported that  $\text{Li}_3\text{AlB}_2\text{O}_6$  is stable unit it melts at  $730^\circ\text{C}$ . On the other hand, Chrysikos *et al.* (11) found that  $\text{Li}_3\text{AlB}_2\text{O}_6$  dissociates to  $\text{Li}_2\text{BaIO}_4$  and  $\alpha\text{-LiBO}_2$  at about  $790^\circ\text{C}$ .

Recently, we reinvestigated this ternary system. Two new monoclinic compounds,  $\text{LiAlB}_2\text{O}_5$  (12) and  $\text{Li}_2\text{AlB}_5\text{O}_{10}$  (13), were synthesized and structurally characterized. A compound with the same chemical composition as  $\text{Li}_3\text{AlB}_2\text{O}_6$  but with a different X-ray powder diffraction pattern was also encountered. Here, we report the synthesis, structure determination, infrared spectra, and thermal stability of this new compound.

## 2. EXPERIMENTAL

A mixture of  $\text{Li}_2\text{CO}_3$ ,  $\text{Al}_2\text{O}_3$ , and  $\text{H}_3\text{BO}_3$  in stoichiometric proportion, 3:1:4, was finely ground and fired at  $690^\circ\text{C}$  in a Pt crucible for 1 or 2 days with one intermediate grinding. Its diffraction measurement was then measured and the process repeated until no further changes could be observed in the powder diffraction pattern.

X-ray powder diffraction measurements on the bulk of product of solid state reaction were performed with an automated Rigaku D/Max-2500 diffractometer (Multilayer Mirror Parallel Beam with High Resolution Soller Slit Optical System) equipped with a graphite monochromator.

<sup>1</sup>To whom correspondence should be addressed. Fax: (008610)82649531. E-mail: xlchen@aphy.iphy.ac.cn.

**TABLE 1**  
**Experimental Details of X-ray Powder Diffraction**  
**and Rietveld Refinement**

Diffractometer	Rigaku D/max2500
Radiation type	CuK $\alpha$
Wavelength ( $\text{\AA}$ )	1.5418
Profile range ( $2\theta$ )	10–85°
Step size ( $2\theta$ )	0.01°
Step scan time per step (s)	16
Number of observations ( $N$ )	7501
Number of contributing reflections	621 ( $K\alpha_1 + K\alpha_2$ )
Number of structure parameters ( $P_1$ )	42
Number of profile parameters ( $P_2$ )	9
$R_B$ (%)	6.87
$R_p$ (%)	6.65
$R_{wp}$ (%)	8.60
$R_{exp}$ (%)	5.08
$S$	1.69

Note.  $R_B = \sum |I_o - I_c| / \sum |I_o|$ ,  $R_p = \sum |y_{io} - y_{ic}| / \sum |y_{io}|$ ,  $R_{wp} = [\sum w_i (y_{io} - y_{ic})^2 / \sum w_i y_{io}^2]^{1/2}$ ,  $R_{exp} = [(N - P_1 - P_2) / \sum w_i y_{io}^2]^{1/2}$ ,  $S = \sum [w_i (y_{io} - y_{ic})^2 / (N - P_1 - P_2)]^{1/2}$ .

Since the sample exhibited a strong tendency of preferred orientation, data were collected in transmission mode. The profile range of data collection was 3°–85° in  $2\theta$ . Only the data in the range of 10°–85° was used in the Rietveld refinement. More technical details can be found in Table 1.

**TABLE 2**  
**Experimental Details of Single-Crystal Data Collection**  
**and Refinement**

Diffractometer	PICKER 4-circle Stoe upgrade diffractometer
Radiation, temperature (K)	CuK $\alpha$ , 293(2)
Wavelength ( $\text{\AA}$ )	1.5418
Absorption	Integration
$T_{min}$ , $T_{max}$	0.794, 0.835
Reflections for refined cell parameters	16
Scan mode	$\omega$ scans
Measured reflections	466
Independent reflections with $I > 2\sigma(I)$	401
Data collection range (°)	$5.81 < \theta < 49.91$
Minimum $h, k, l$	–4, –5, 0
Maximum $h, k, l$	4, 6, 7
Reflections used in the last refinement	466
Weighting scheme	$w = 1/[\sigma^2(F_o^2) + (0.0400P)^2 + 0.2800P]$ where $P = (F_o^2 + 2F_c^2)/3$
Number of refined parameters	84
Max $\Delta/\sigma$	< 0.001
Reliability factor $R_1$ ; $wR_2$	0.0306, 0.0777
Goodness of fit	1.224
$\Delta\rho_{max}$ ( $e \text{\AA}^{-3}$ )	0.232
$\Delta\rho_{min}$ ( $e \text{\AA}^{-3}$ )	–0.281

Single-crystal diffraction data were collected with a PICKER four-circle Stoe upgrade diffractometer. The crystal used for collecting the data (about  $0.07 \times 0.06 \times 0.03$  mm in size) was selected from the product of the solid state reaction. Additional technical details are given in Table 2.

Infrared spectra were recorded with a Perkin–Elmer 983 infrared spectrophotometer in the 200 to  $1500\text{-cm}^{-1}$  wavenumber range using KBr pellets. A CP-G differential thermal instrument was employed to perform DTA and TGA experiments. The heating rate was  $10^\circ\text{C}/\text{min}$  in the temperature range from room temperature ( $23^\circ\text{C}$ ) to  $1024^\circ\text{C}$ .

### 3. RESULTS AND DISCUSSION

The unit cell of the title compound was first determined from the powder diffraction pattern using the Dicvol91 program (14). All the reflections before  $40^\circ$  in  $2\theta$  except for

**TABLE 3**  
**List of Indexes,  $d$  Values, and Diffraction Intensities**  
**of  $\text{Li}_3\text{AlB}_2\text{O}_6$**

$h$	$k$	$l$	$d_{obs}$	$d_{cal}$	$I_{obs}$
0	0	1	7.636	7.629	5
	*		6.240		3
0	1	0	5.970	5.967	26
0	1	1	5.465	5.463	10
1	0	0	4.881	4.878	16
0	–1	1	4.1873	4.1875	22
1	0	1	4.1243	4.1236	22
–1	0	1	4.098	4.096	3
0	0	2	3.8137	3.8143	5
1	1	0	3.7864	3.7862	14
0	1	2	3.6939	3.6939	27
1	1	1	3.6569	3.6568	28
	*		3.2225		7
1	–1	1	3.1775	3.1782	19
0	2	1	3.0717	3.0716	6
–1	0	2	2.9939	2.9941	8
1	1	2	2.9593	2.9595	35
–1	1	2	2.9301	2.9304	20
0	–1	2	2.8823	2.8827	9
0	2	2	2.7314	2.7317	100
0	1	3	2.6046	2.6043	13
0	–2	1	2.5556	2.5562	12
0	0	3	2.541	2.543	15
1	–2	0		2.540	
–1	2	0		2.540	
1	–1	2	2.483	2.485	21
–1	–1	2	2.4779	2.4783	46
2	0	0	2.4390	2.4391	39
1	2	2	2.3935	2.3936	3
2	0	1	2.3281	2.3282	3
–2	0	1	2.3180	2.3183	3
2	1	0	2.2620	2.2618	15
1	0	3		2.2618	

Note. \*Reflections of  $\text{Li}_2\text{AlBO}_4$ .

**TABLE 4**  
Crystal Data

	This work	Ref. (9)
Formula	$\text{Li}_3\text{AlB}_2\text{O}_6$	$\text{Li}_6\text{Al}_2(\text{BO}_3)_4$
Symmetry	Triclinic	Triclinic
Space group	$P\bar{1}$	$P\bar{1}$
$a$ (Å)	4.876(8)	6.131(2)
$b$ (Å)	6.191(16)	4.819(1)
$c$ (Å)	7.910(20)	8.227(3)
$\alpha$ (°)	74.46(18)	90.3(0)
$\beta$ (°)	89.44(17)	117.0(0)
$\gamma$ (°)	89.52(18)	89.9(0)
Volume (Å <sup>3</sup> )	230.0(9)	216.5
$Z$	2	1
$D_x$ (gc m <sup>-3</sup> )	2.388	2.537
Molecular weight	165.42	330.84
Color	Colorless	—

**TABLE 5**  
Fractional Atomic Coordinates and Equivalent Isotropic Displacement Parameters (Å<sup>2</sup>)

	$x$	$y$	$z$	$U_{\text{eq}}$
Al	0.1491(2)	0.5509(2)	− 0.72632(14)	0.0106(4)
B1	− 0.1588(9)	0.8207(7)	− 0.5711(5)	0.0103(11)
B2	0.6654(9)	0.6723(7)	− 0.9091(6)	0.0110(11)
O1	0.1098(5)	0.7555(4)	− 0.6054(3)	0.0121(7)
O2	− 0.2897(5)	0.9899(4)	− 0.6807(3)	0.0125(7)
O3	− 0.2734(5)	0.7039(4)	− 0.4107(3)	0.0134(7)
O4	0.3797(5)	0.6621(4)	− 0.8937(3)	0.0135(7)
O5	0.8121(5)	0.5112(4)	− 0.7840(3)	0.0124(7)
O6	0.7909(5)	0.8340(4)	− 0.0308(3)	0.0138(7)
Li1	− 0.3339(13)	0.2594(11)	− 0.6096(8)	0.017(2)
Li2	− 0.1780(14)	0.1106(11)	− 0.9260(8)	0.020(2)
Li3	0.6736(14)	0.9777(12)	− 0.2558(9)	0.024(2)

Note.  $U_{\text{eq}} = \frac{1}{3} \sum_i \sum_j U_{ij} a_i^* a_j^* a_i a_j$ . The thermal parameters of B and Li atoms are  $U_{\text{iso}}$ .

two weak ones of  $\text{Li}_2\text{AlBO}_4$  can be indexed based on a triclinic unit cell with high figures of merits:  $M(28) = 58.2$  (15),  $F(28) = 119.0(0.0055, 43)$  (16). The lattice parameters deduced from the powder diffraction pattern are  $a = 4.8784(4)$  Å,  $b = 6.1936(8)$  Å,  $c = 7.9181(8)$  Å,  $\alpha = 74.467(9)^\circ$ ,  $\beta = 89.481(9)^\circ$ , and  $\gamma = 89.582(16)^\circ$ . The results of the indexation are presented in Table 3. The single-crystal analysis gave almost the same unit cell with lattice parameters  $a = 4.876(8)$  Å,  $b = 6.191(16)$  Å,  $c = 7.910(20)$  Å,  $\alpha = 74.46(18)^\circ$ ,  $\beta = 89.44(17)^\circ$ , and  $\gamma = 89.52(18)^\circ$ . Since these six cell parameters were refined on only 16 reflections in single-crystal analysis, the standard deviations of cell parameters are quite big. The structure was routinely solved and refined with the *SHELXTL PLUS* (17) program package. The crystal data are given in Table 4. For comparison, Abdullaev *et al.*'s results published in Ref. (9) are also presented in this table. The fractional atomic coordinates and equivalent isotropic displacement parameters are reported in Table 5. Anisotropic displacement parameters and some important geometric parameters are listed in Tables 6 and 7, respectively.

To prove that the single crystal used in the structure analysis was indeed representing the bulk material, a Rietveld refinement was performed on the X-ray powder diffraction data using a *DBWS9411* program (18). The background intensities were obtained by linear interpolation between selected points in the pattern. Thermal parameters were set to be the same as those values obtained in the single-crystal data analysis and were not refined. Weak reflections resulting from a small impurity of  $\text{Li}_2\text{BO}_4$  were left as “errors” and were not included as a second phase. A total of 42 structural parameters and 9 profile parameters were refined. The refinement finally converged to agreement factors of  $R_B = 6.87\%$ ,  $R_p = 6.65\%$ , and  $R_{wp} = 8.60\%$  with  $R_{\text{exp}} = 5.08\%$ . The details of the Rietveld refinement are presented in Table 1 and the final refinement pattern is given in Fig. 1. Lattice constants were refined to  $a = 4.8771(0)$  Å,  $b = 6.1914(0)$  Å,  $c = 7.9143(0)$  Å,  $\alpha = 74.465(2)^\circ$ ,  $\beta = 89.4780(3)^\circ$ , and  $\gamma = 89.5826(4)^\circ$ . The positional parameters obtained by the Rietveld refinement are listed in Table 8. They differ little with respect to the single-crystal refinement, but the estimated standard deviations

**TABLE 6**  
Anisotropic Displacement Parameters (Å<sup>2</sup>)

	$U_{11}$	$U_{22}$	$U_{33}$	$U_{23}$	$U_{13}$	$U_{12}$
Al	0.0067(7)	0.0112(7)	0.0121(7)	0.0000(5)	0.0011(5)	0.0006(5)
O1	0.0046(14)	0.0159(14)	0.0136(15)	− 0.0004(11)	0.0008(11)	− 0.0005(11)
O2	0.012(2)	0.0118(14)	0.0117(15)	0.0000(11)	0.0008(11)	0.0015(11)
O3	0.0076(14)	0.016(2)	0.0138(14)	0.0016(12)	0.0017(11)	0.0014(12)
O4	0.0064(15)	0.017(2)	0.014(2)	0.0004(12)	0.0021(11)	0.0001(12)
O5	0.0072(14)	0.0128(15)	0.0145(14)	0.0009(11)	− 0.0012(11)	0.0000(11)
O6	0.0093(14)	0.0145(14)	0.0152(14)	0.0001(11)	0.0017(11)	− 0.0011(11)

**TABLE 7**  
Selected Geometric Parameters (Å, °)

A1–O4	1.728(5)	Li1–O5 <sup>i</sup>	1.920(8)
A1–O5 <sup>i</sup>	1.746(4)	Li1–O3 <sup>v</sup>	1.937(7)
A1–O3 <sup>ii</sup>	1.764(5)	Li1–O1 <sup>ii</sup>	2.011(8)
A1–O1	1.789(5)	⟨Li1–O⟩	1.944(8)
⟨A1–O⟩	1.757(5)	Li2–O2 <sup>iv</sup>	1.956(9)
B1–O2	1.330(6)	Li2–O6 <sup>iv</sup>	1.932(8)
B1–O3	1.395(6)	Li2–O4 <sup>vii</sup>	1.978(9)
B1–O1	1.412(6)	Li2–O6 <sup>viii</sup>	2.100(9)
⟨B1–O⟩	1.379(6)	⟨Li2–O⟩	1.992(9)
B2–O6 <sup>iii</sup>	1.336(6)	Li3–O6	1.857(9)
B2–O4	1.398(6)	Li3–O2 <sup>ix</sup>	1.938(8)
B2–O5	1.400(6)	Li3–O1 <sup>x</sup>	2.021(9)
⟨B2–O⟩	1.378(6)	Li3–O3 <sup>xi</sup>	2.354(9)
Li1–O2 <sup>iv</sup>	1.908(8)	⟨Li3–O⟩	2.043(9)
O4–A1–O5 <sup>i</sup>	117.8(2)	O2–B1–O3	121.9(4)
O4–A1–O3 <sup>ii</sup>	110.9(2)	O2–B1–O1	122.2(4)
O5 <sup>i</sup> –A1–O3 <sup>ii</sup>	108.6(2)	O3–B1–O1	115.8(4)
O4–A1–O1	106.1(2)	O6 <sup>iii</sup> –B2–O4	121.7(4)
O5 <sup>i</sup> –A1–O1	102.6(2)	O6 <sup>iii</sup> –B2–O5	122.0(4)
O3 <sup>iii</sup> –A1–O1	110.4(2)	O4–B2–O5	116.2(4)

Note. Symmetry codes: (i)  $x - 1, y, z$ ; (ii)  $-x, 1 - y, -1 - z$ ; (iii)  $x, y, z - 1$ ; (iv)  $x, y - 1, z$ ; (v)  $-1 - x, 1 - y, -1 - z$ ; (vi)  $1 - x, 1 - y, -1 - z$ ; (vii)  $-x, 1 - y, -2 - z$ ; (viii)  $x - 1, y - 1, z - 1$ ; (ix)  $-x, 2 - y, -1 - z$ ; (x)  $1 - x, 2 - y, -1 - z$ ; (xi)  $1 + x, y, z$ .

are somewhat larger. The fact that the two independent structure refinements gave essentially the same result adds further weight to the correctness of the crystal analysis.

As shown in Fig. 2, every  $\text{BO}_3$  group connected with two  $\text{AlO}_4$  tetrahedra through oxygen atoms to form infinite

**TABLE 8**  
Atomic Coordinates Obtained by Rietveld Refinement

Atom	x	y	z
A1	0.1506(5)	0.5504(4)	−0.7279(3)
B1	−0.161(2)	0.822(1)	−0.569(1)
B2	0.667(2)	0.672(1)	−0.910(1)
O1	0.1131(8)	0.7567(7)	−0.6043(5)
O2	−0.2896(7)	0.9963(6)	−0.6838(5)
O3	−0.2766(7)	0.6988(6)	−0.4084(5)
O4	0.3818(8)	0.6669(6)	−0.8933(5)
O5	0.8141(8)	0.5089(7)	−0.7856(5)
O6	0.7881(8)	0.8401(6)	−0.0350(5)
Li1	−0.347(2)	0.264(2)	−0.597(2)
Li2	−0.167(2)	0.117(2)	−0.932(1)
Li3	0.680(2)	0.954(2)	−0.255(2)

$[\text{Al}_2(\text{BO}_3)_4]_\infty^{6-}$  complex chains that run along the  $a$  axis. The unique configuration of  $\text{AlO}_4$  and  $\text{BO}_3$  groups was also found in the structure determined by Abdullaev and Mamedov (8,9). In their structure, these  $[\text{Al}_2(\text{BO}_3)_4]_\infty^{6-}$  chains run parallel to the  $b$  axis (see Figs. 3a and 3c). However, the Li atoms have a different distribution in the two structures. In both cases the Li atoms are tetrahedrally coordinated by oxygen atoms and are shown as medium gray tetrahedra in Figs. 3b and 3d. In the structure found by Abdullaev *et al.* the Li tetrahedra are clustered and shares edges with both the Al tetrahedra and other Li tetrahedra and with the  $\text{BO}_3$  groups. In contrast, in the structure presented here, the Li tetrahedra are distributed more evenly

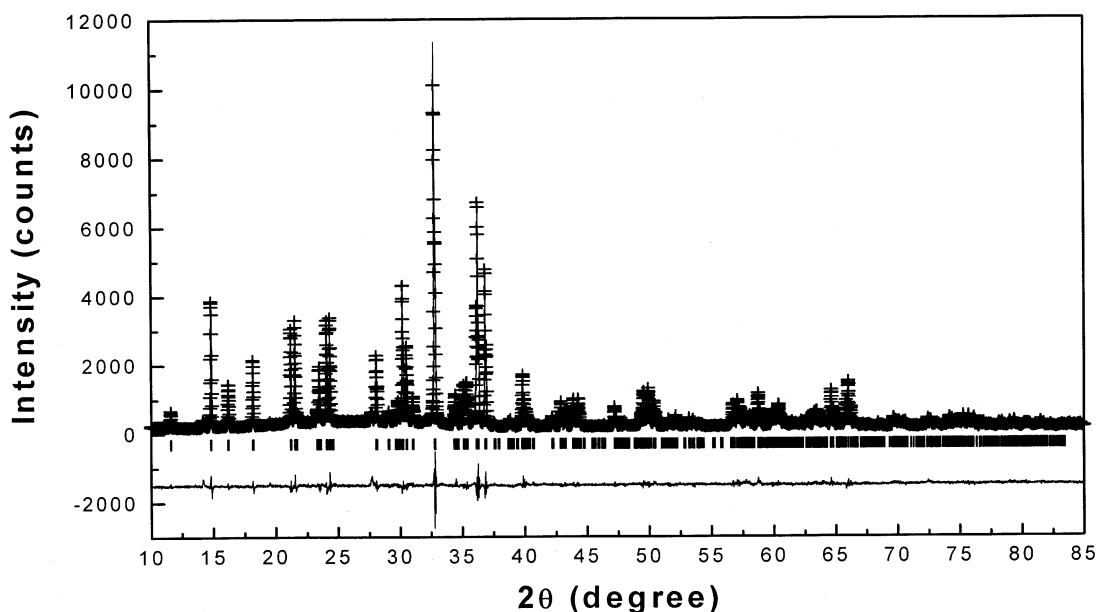


**FIG. 1.** The final Rietveld refinement plots of the  $\text{Li}_3\text{AlB}_2\text{O}_6$ . Small crosses (+) correspond to experimental values and the continuous line the calculated pattern; vertical bars (|) indicate the positions of Bragg peaks. The bottom trace depicts the difference between the experimental and the calculated intensity values.

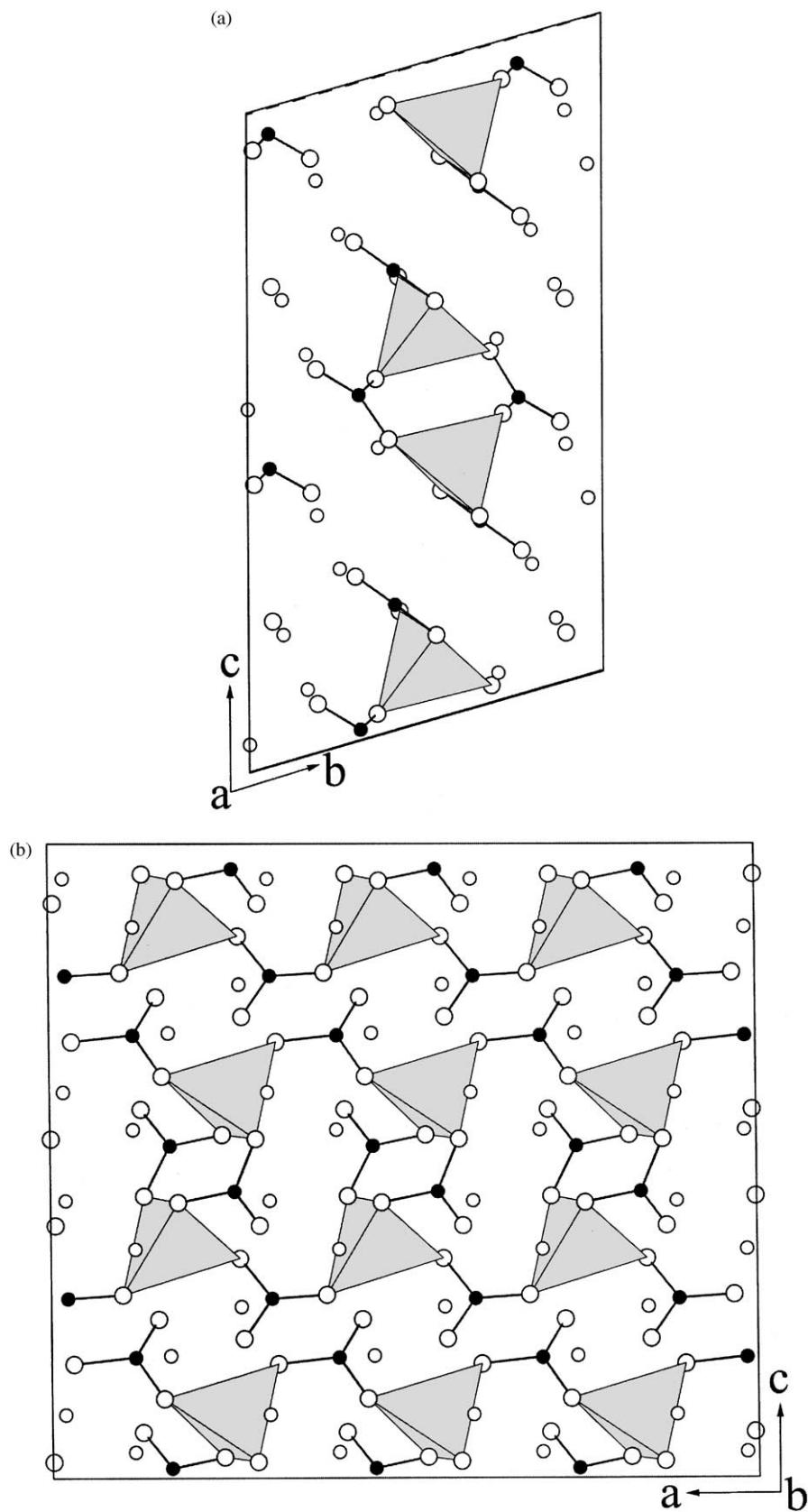


**FIG. 2.** The structure projection of  $\text{Li}_3\text{AlB}_2\text{O}_6$  along the  $a$  axis (a) and the  $b$  axis (b). Tetrahedra represent  $\text{AlO}_4$  groups. Big open circles depict O atoms, small ones Li atoms, and solid ones B. To show the structural characteristics clearly, more than a unit cell was presented here.

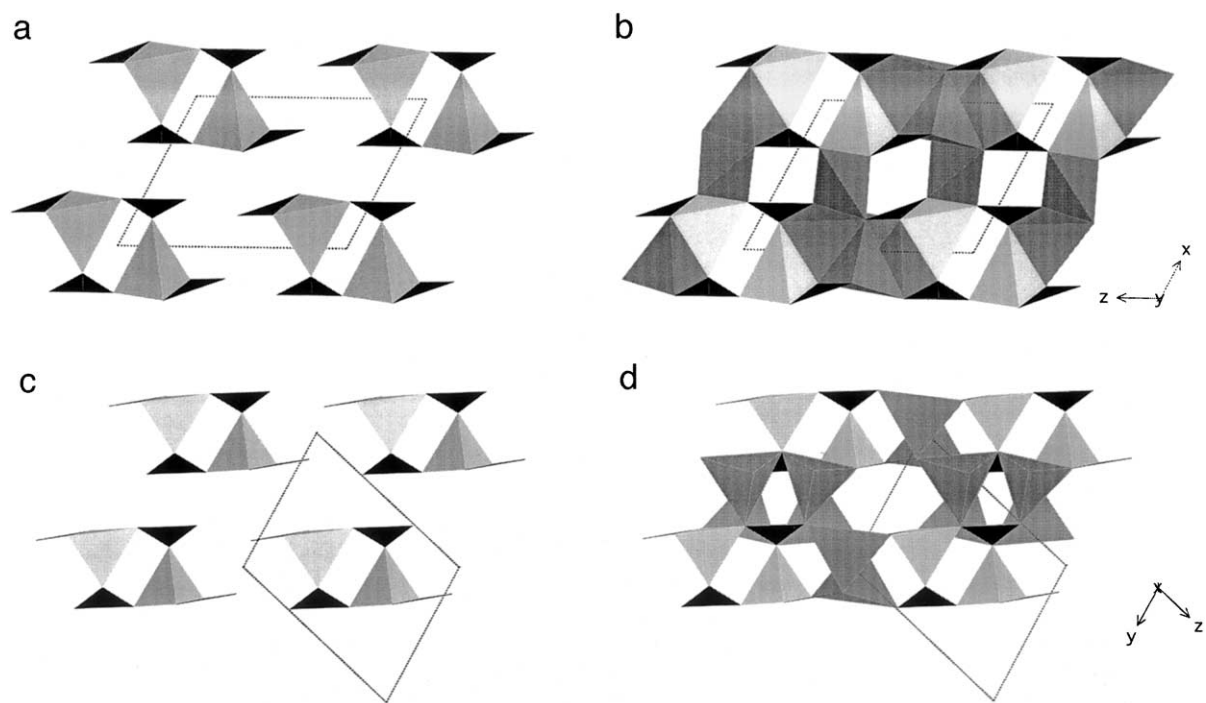


**FIG. 3.** Comparison between the structure determined by Abdullaev *et al.* and the structure presented here. (a) and (b) are projections of the structure determined by Abdullaev *et al.* while (c) and (d) are projections of the structure presented here. Only  $\text{AlO}_4$  tetrahedra (gray polyhedra) and  $\text{BO}_3$  groups (black triangles) are shown in (a) and (c) for clarity. Darker polyhedra in (b) and (d) are Li–O groups.

between the chains and are only connected with  $\text{AlO}_4$  and  $\text{BO}_3$  groups through corners. These differences in the structures are also reflected in the cell parameters and naturally in the powder diffraction patterns of the two structures (Fig. 4). It is also important to point out that the triclinic cell of Abdullaev *et al.* cannot be transformed into the cell found in this work.

The bond valences have also been calculated according to the Brown and Altermatt parameters (19) for both structures reported in the present work and Ref. (9) and are listed in Tables 9 and 10, respectively. It can be seen that in our structure the bond valence sums are very reasonable for both cations and oxygens. Especially, the bond valence sum for the Al atom is 3.01, which is quite different from the value of 2.11 found in the structure of Abdullaev *et al.*

The infrared spectra of this structure are given in Fig. 5. Because this structure is related to the one determined by Abdullaev *et al.* (8,9), its infrared spectra also show many

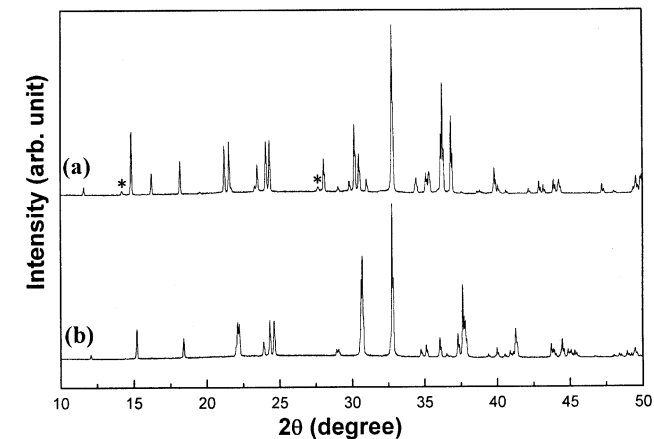


**FIG. 4.** X-ray powder diffraction patterns of the  $\text{Li}_3\text{AlB}_2\text{O}_6$ . (a) Experimental data of the structure determined in this study. (b) Calculated pattern of the structure reported by Abdullaev *et al.* Asterisks indicate reflections of the impurity of  $\text{Li}_2\text{AlBO}_4$ .

**TABLE 9**  
**Li–O, Al–O, and B–O Bond Valence in  $\text{Li}_3\text{AlB}_2\text{O}_6$  Calculated Using the Structural Data Presented in This work**

	O1	O2	O3	O4	O5	O6	$\Sigma S$
Li1	0.229	0.303	0.280		0.293		1.11
Li2		0.266		0.250		0.180/0.283	0.98
Li3	0.223	0.279	0.091			0.348	0.94
Al	0.689		0.737	0.812	0.774		3.01
B1	0.895	1.117	0.937				2.95
B2				0.930	0.925	1.099	2.86
$\Sigma S$	2.04	1.97	2.05	1.99	1.99	1.91	

*Note.* Bond valence parameters were cited from Ref. (19) and B was set to be 0.37.

**TABLE 10**  
**Li–O, Al–O, and B–O Bond Valences in  $\text{Li}_6\text{Al}_2(\text{BO}_3)_4$**   
**Calculated Using the Structural Data Reported in Ref. (9)**

	O1	O2	O3	O4	O5	O6	$\Sigma S$
Li1		0.323	0.287/ 0.303	0.344			1.26
Li2		0.308	0.253	0.263	0.329		1.15
Li3	0.331		0.162	0.241		0.382	1.12
Al	0.598	0.549			0.388	0.573	2.11
B1		0.999	0.933			0.956	2.89
B2	1.091			0.948	0.896		2.94
$\Sigma S$	2.02	2.18	1.94	1.80	1.61	1.91	

Note. Bond valence parameters were cited from Ref. (19) and B was set to be 0.37.

similarities to the results of Chrysikos *et al.* (11). The most significant differences occur at the following frequencies: the peak at about  $1400\text{ cm}^{-1}$  has split into two peaks at  $1366$  and  $1415\text{ cm}^{-1}$ , respectively; the active vibration at about  $480\text{ cm}^{-1}$  is almost as strong as the one at about  $530\text{ cm}^{-1}$ ; the peak at about  $620\text{ cm}^{-1}$  has developed into a well-defined doublet with maxima at  $595$  and  $618\text{ cm}^{-1}$ . These dissimilarities in the infrared spectra may reflect the differences in their structures.

The results of DTA and TGA are shown in Fig. 6. No weight loss was detected between room temperature and  $1024^\circ\text{C}$ . In this interval, two endothermic peaks with maxima at  $804$  and  $859^\circ\text{C}$  were observed. The sample used in the DTA experiments was found to be somewhat melted. X-ray powder diffraction analysis indicated that the cooled melt was composed of  $\text{Li}_3\text{AlB}_2\text{O}_6$ ,  $\text{Li}_2\text{AlBO}_4$ ,  $\alpha\text{-LiBO}_2$ , and  $\gamma\text{-LiAlO}_2$ . An additional sample prepared by quenching the melt of  $\text{Li}_3\text{AlB}_2\text{O}_6$  from  $900^\circ\text{C}$  in cool water mainly consists of amorphous phase and  $\gamma\text{-LiAlO}_2$ . According to these results and referring to Chrysikos *et al.*'s report (11), we

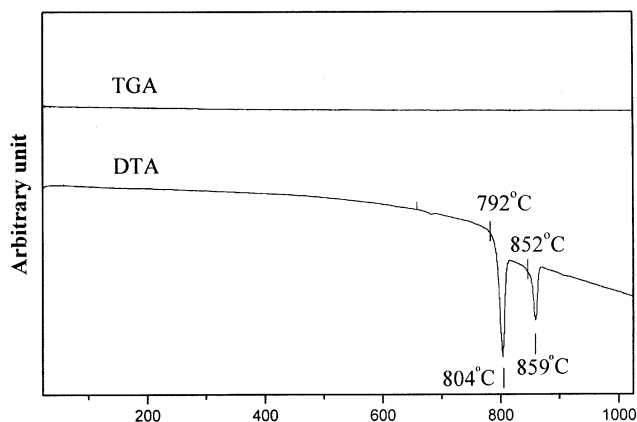


**FIG. 6.** TGA and DTA curves of  $\text{Li}_3\text{AlB}_6$ .

propose a tentative explanation for the two endothermic peaks observed in the DTA curve: at about  $792^\circ\text{C}$  the title compound first dissociates into  $\text{Li}_2\text{AlBO}_4$  and  $\alpha\text{-LiBO}_2$ , and then, at about  $852^\circ\text{C}$ ,  $\text{Li}_2\text{AlBO}_4$  further dissociates into  $\gamma\text{-LiAlO}_2$  and a liquid with the composition of  $\text{LiBO}_2$ . This result is in agreement with that of Chrysikos *et al.* (11) except for the dissociation temperature of  $\text{Li}_2\text{AlBO}_4$ . We think that our results is more reasonable because  $\alpha\text{-LiBO}_2$  is reported to melt at about  $850^\circ\text{C}$  (20, 21) (S. Zhao, thesis for Master's degree, Institute of Physics, Chinese Academy of Sciences, 1987). Therefore, it is not possible that  $\text{Li}_2\text{AlBO}_4$  dissociates into  $\gamma\text{-LiAlO}_2$  and  $\alpha\text{-LiBO}_2$  at about  $890^\circ\text{C}$ .

It is interesting to note that the crystal used for solving the structure in this work was selected from the product of solid state reaction at  $690^\circ\text{C}$  while Abdullaev *et al.* got their crystal from a melt of the system of  $\text{LiBO}_2\text{--Al}_2\text{O}_3$  at  $785^\circ\text{C}$ . This might be the reason why we got a structure of  $\text{Li}_3\text{AlB}_2\text{O}_6$ , which is different from the one reported by Abdullaev *et al.* However, in the course of the investigation of the thermal stability of  $\text{Li}_3\text{AlB}_2\text{O}_6$ , we never observed the powder diffraction evidence of the structure reported by Abdullaev *et al.* (7). In addition, the results reported here are also further supported by our systematic research in the  $\text{Li}_2\text{O--Al}_2\text{O}_3\text{--B}_2\text{O}_3$  ternary system.

#### 4. CONCLUSIONS

In this work we have synthesized a new compound,  $\text{Li}_3\text{AlB}_2\text{O}_6$ , by solid state reaction and solved its structure from single-crystal diffraction data. The structure was further verified by Rietveld refinement on the powder diffraction data. It was found that this structure was composed of infinite  $[\text{Al}_2(\text{BO}_3)_4]_\infty^{6-}$  complex chains that run along the  $a$  axis and Li atoms in tetrahedral coordination, connecting these chains through vertices. The structure reported here is significantly different from that determined by Abdullaev *et al.*

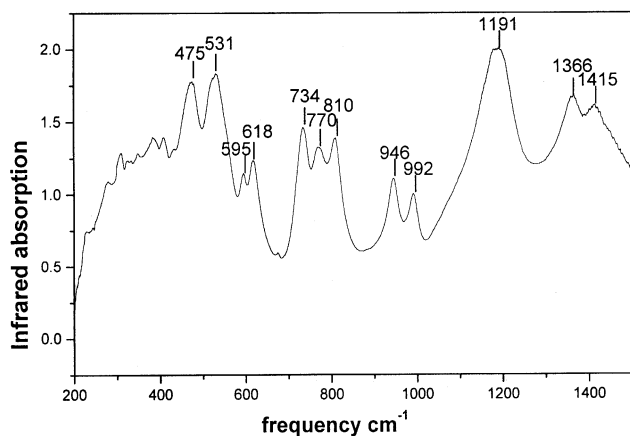


**FIG. 5.** Infrared spectra of title compound.

Infrared spectra and thermal analysis are also reported and compared with previous results. Because of common features in the structures, the IR spectra of the title compound exhibit many similarities to spectra reported previously in the literature. Based on the experimental results and previous reports, a tentative interpretation is proposed for the thermal stability of the title compound: this compound first dissociates into  $\text{Li}_2\text{AlBO}_4$  and  $\alpha\text{-LiBO}_2$  at about  $792^\circ\text{C}$  and then the  $\text{Li}_2\text{AlBO}_4$  further dissociates into  $\gamma\text{-LiAlO}_2$  and a liquid with the composition of  $\text{LiBO}_2$  at about  $852^\circ\text{C}$ .

#### ACKNOWLEDGMENTS

We would like to thank Prof. G. L. Lü of Zhejiang University and Mr. Mitsunaga Tiru of Rigaku Corporation Application Laboratory for their great help in collecting X-ray powder diffraction data and Ms. Y. P. Xu and Mr. T. Xu for their technical help. This work was financially supported by the National Natural Science Foundation of China and the Chinese Academy of Sciences.

#### REFERENCES

1. C. Chen, B. Wu, A. Jiang, and G. You, *Sci. Sinica B* **28**, 235 (1985).
2. C. Chen, Y. Wu, A. Jiang, B. Wu, G. You, R. Li, and S. Lin, *J. Opt. Soc. Am. B* **6**, 616 (1989).
3. Y. Wu, T. Sasaki, S. Nakai, A. Yokotani, H. Tang, and C. Chen, *Appl. Phys. Lett.* **62**, 2614 (1993).
4. C. Chen, Y. Wang, B. Wu, K. Wu, W. Zeng, and L. Yu, *Nature* **373**, 322 (1995).
5. Z. Hu, T. Higashiyama, M. Yoshimura, Y. Mori, and T. Sasaki, *Z. Kristallogr.* **214**, 433 (1999).
6. K. H. Kim and F. A. Hummel, *J. Am. Ceram. Soc.* **45**, 487 (1962).
7. G. Abdullaev, P. Rza-zade, and K. Mamedov, *Russ. J. Inorg. Chem.* **28**, 428 (1983). [English translation]
8. G. Abdullaev and K. Mamedov, *Kristallografiya* **19**, 165 (1974).
9. G. Abdullaev and K. Mamedov, *Kristallografiya* **27**, 381 (1982).
10. J. Åhman, G. Svensson, and J. Grins, *Acta Chem. Scand* **51**, 1045 (1997).
11. G. Chrysikos, M. Bitsis, J. Kapoutsis, and E. Kamitsos, *J. Non-Cryst. Solids* **217**, 278 (1997).
12. M. He, X. L. Chen, Y. C. Lan, H. Li, and Y. P. Xu, *J. Solid State Chem.* **156**, 181 (2001).
13. M. He, H. Li, X. L. Chen, Y. P. Xu, and T. Xu, *Acta Crystallogr. C* **57**, 1010 (2001).
14. A. Boulton and D. Louer, *J. Appl. Crystallogr.* **24**, 987 (1991).
15. P. M. de Wolff, *J. Appl. Crystallogr.* **5**, 108 (1968).
16. G. S. Smith and R. L. Snyder, *J. Appl. Crystallogr.* **12**, 60 (1979).
17. SHELXTL PLUS, Siemens Analytical X-Ray Instruments Inc., Madison, WI, 1990.
18. D. A. Wiles and R. A. Young, *J. Appl. Crystallogr.* **14**, 149 (1981).
19. I.D. Brown and D. Altermatt, *Acta Crystallogr. B* **41**, 244 (1985).
20. A. P. Rollet and R. Bouaziz, *Compt. Rend.* **240**, 2417 (1955).
21. B. S. R. Sastry and F. A. Hummel, *J. Am. Ceram. Soc.* **41**, 7 (1958).